Revista Facultad de Ingeniería, October 27, 2020

Automated Design of an Induction Stove with On-Grid Photovoltaic Support

Diseño automatizado de una cocina de inducción con soporte fotovoltaico On-Grid

Authors: ***Double-blind review***

KEYWORDS:
induction stove, control, energy, toquilla straw

estufa de inducción, control, energíia, paja toquilla

ABSTRACT: The design of an induction stove to reduce the use of firewood in the toquilla straw cooking process is presented. The induction stove requires a resonance frequency around 31 kHz to work, a full-bridge inverter is designed to achieve the operating frequency. Next, a state space model of the thermal system composite by an induction hob is used to temperature control by mean a PID. Finally, an ON-GRID photovoltaic (PV) system is designed to generate the stove energy demanded.

RESUMEN: Se presenta el diseño de una estufa de inducción para reducir el uso de leña en el proceso de cocción de la paja toquilla. La estufa de inducción requiere una frecuencia de resonancia de aproximadamente 31kHz para funcionar, se diseña un inversor de puente completo para lograr la frecuencia de operación. A continuación, se utiliza un modelo de espacio de estados del sistema térmico compuesto por una placa de inducción para controlar la temperatura mediante un PID. Finalmente, se diseña un sistema fotovoltaico ON-GRID para generar la energía demandada de la estufa.

1. Introduction

The productive processes technification is an important topic for technical and economic Colombian development. Currently, there are many processes that are realized handcrafted whereby the production amount is low. The iraca palm or straw toquilla is a natural resource exploited by peasant families in Linares-Nariño. The production derived from this plant has managed to form a social and cultural fabric that that has highlighted linares in Nariño. Within the production of toquilla straw the raw material is the vegetable fiber and five links are described starting from the cultivation, palm processing, commercialization of vegetable fiber, weaving, and commercialization of handicrafts. These stages of production over the years have been worked in an artisanal way, whose experience has been inherited from generation to generation.

In the palm processing health risks are more evident. First, cooking of toquilla fibers requires high temperature which lasts around four hours according to the local producers. Due to this processing is realized with traditional methods like firewood combustion, the generation of CO2 has caused respiratory problems for the peopple incharge, as well as air pollution. Furthermore, the demand for induction stoves or grills has increased considerably, as various companies have opted for their high performance. Countries like Ecuador have developed policies to encourage the use of these devices, thus generating energy subsidies that present a zero rate for consumption of up to 80 kilowatt hours (kW / H) [1]. Induction heating has been applied to different industrial processes such as the work carried out by [2], where the control of thermal behavior for inductive heating towards a fluid is studied, in order to obtain optimum temperature levels. On the other hand, some studies seek to improve the stove's heat system increasingly as in [3], likewise the studies addressed for optimal temperature control are highlighted like [4].

2. Operation of an induction stove

Induction cookers are based on the conversion of electrical energy into electromagnetic energy to generate heat in a container. This is achieved by means of a resonant electronic circuit which generates an oscillating magnetic field through a coil which will induce the magnetic field in a container with ferromagnetic properties such as iron or ferromagnetic steel. The induced magnetic field generates eddy currents and losses of the Joule effect which cause the container heat up and its contents [5]. In this way by controlling the oscillat-

ing magnetic field it is possible to control the amount of heat to the container instantly [5], [6].
The figure 1 shows the detailed block diagram of an induction stove.

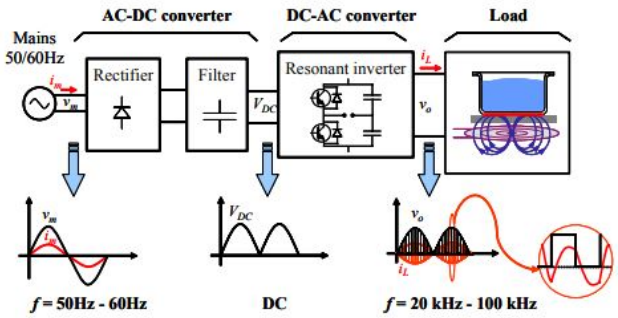

Figure 1 Schematic electronic circuit of an induction stove [7]

3. Resonant inverter

A resonant inverter generate a voltage or current wave with a certain magnitude and frequency from a continuous source. This type of inverter generates a high frequency square wave (greater than 20KHz), next the wave is filtered by a resonant tank circuit in order to obtain a high frequency wave free of harmonics at the output [8], the figure 2 present a block diagram of a resonant inverter.

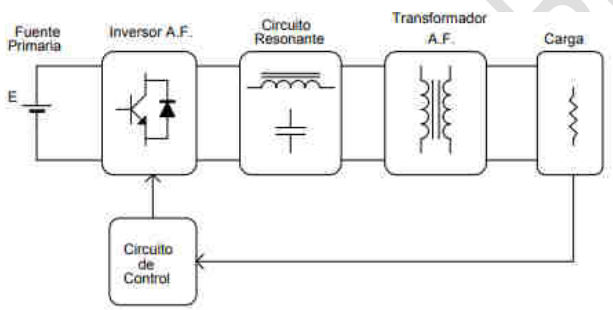

Figure 2 Block diagram of a resonant inverter [8]

3.1 Stove parameters

A series full bridge inverter is used as resonant inverter, the figure 3 shows the schematic circuit. The load is a LC branch with $L = 20\mu H$ and $C = 7\mu F$, the input voltage is $V_{in} = 100V$ and the current over the LC load is $I_o = 31,25A$. The transistor switching is perform by a PWM with a frequency of $31,25kHz$, this allow that the system achieve the resonant frequency to to warm the water for the toquilla straw process.

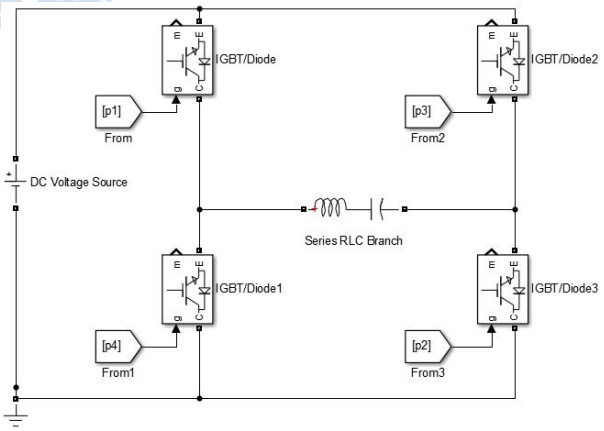

Figure 3 Schematic of a series full bridge inverter with LC load

The resonant inverter is simulated in Simulink of MATLAB, the voltage result is presented in the figure 4. The peak voltage is $125V$ and the frequency is $33,3kHz$ that is according to expectations. Moreover, even though the voltage does not have a sinusoidal shape, its use is possible. Besides, the apparent power demanded by the inductive load is presented in figure 5, this power has a maximum value of $3671W$.

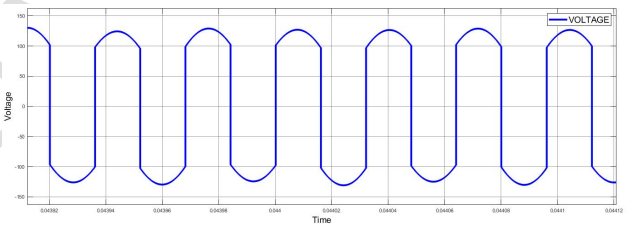

Figure 4 Voltage over the $20\mu H$ coil

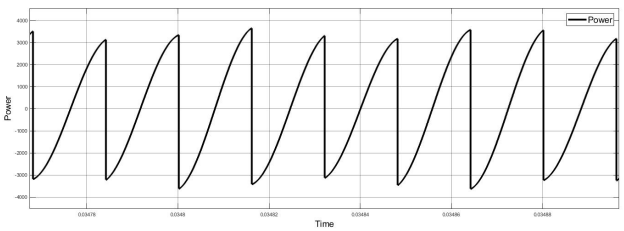

Figure 5 Comportamiendo de potencia activa y reactiva presente en la salida del inversor.

4. Dynamical model of the induction stove

In equation (1) the dynamical model of an induction stove is presented. This model is used to implement a

temperature control that ensure the stability and regulation of the system.

$$\begin{cases} C_{COIL}\dot{T}_{COIL} = (1-K_1)P - (h_{CA}+ h_{GC})T_{COIL} + h_{GC}T_{GLASS} + h_{CA}T_{AIR} \\ C_{GLASS}\dot{T}_{GLASS} = -(h_{GA}+h_{GC}+ h_{PG})T_{GLASS} + h_{PG}T_{POT} + h_{GC}T_{COIL}+ h_{GA}T_{AIR} \\ C_{POT}\dot{T}_{POT} = K_1P - (h_{PA}+h_{PG}+h_{PW})T_{POT} +h_{PW}T_{water} + h_{PG}T_{GLASS} + h_{PA}T_{AIR} \\ M_{water}CW\dot{T}_{water} = -(h_{WA}+h_{PW})T_{water}+ h_{PW}T_{POT} + h_{WA}T_{AIR} + \dot{M}_{water}h_{vs}(P_{est}) \end{cases} \quad (1)$$

Where:

- C_{coil} is the equivalent thermal capacity of the coil
- C_{glass} is the equivalent thermal capacity of the glass
- C_{pot} is the equivalent thermal capacity of the pot
- C_W is the water specific thermal capacity
- T_{COIL} is the coil temperature
- T_{GLASS} is the glass temperature
- T_{POT} is the pot temperature
- T_{WATER} is the water temperature
- M_{WATER} is the water mass
- P is the total active power absorbed at the coil
- h_{CA} represents the heat transfer coefficient coil to air multiplied by the relative surface
- h_{GA} represents the heat transfer coefficient glass to air multiplied by the relative surface
- h_{PA} is the heat transfer coefficient pot to air multiplied by the relative surface
- h_{WA} is the heat transfer coefficient water to air multiplied by the relative surface
- h_{GC} is the heat transfer coefficient glass to coil multiplied by the relative surface
- h_{PG} is the heat transfer coefficient pot to glass multiplied by the relative surface
- h_{PW} is the heat transfer coefficient pot to water multiplied by the relative surface

According to [9] the model provides an estimate of different temperatures, these being Tcoil, Tglass, Tpot, Twater. This work takes the temperature variation in the container (Tpot) to be controlled. Taking as reference the work in [9] as well as specialists in the subject, the values of these constants were selected for the simulations. Finally, the value of the constants was adjusted taking into account the real behavior of the stove (artisan process) that was observed during a visit to Linares. Considering this, the numerical value of each coefficient is presented below:

- Ccoil = 0.092
- Cglass = 0.200
- Cpot = 0.12
- CW = 4.184
- hCA = 0.2
- hGA = 0.34
- hPA = 1
- hWA = 0.1
- hGC =0.4
- hPG = 0.82
- hPW = 0.3
- k1 = 4.7

4.1 State Space Model

From the dynamic model described in the equation 1, the representation in state space is made with the power (P) absorbed by the coil as the system input and the temperature of the container (T_{pot}) as the only output. Assuming, $\dot{T}_{COIL} = \dot{x}_1$, $\dot{T}_{GLASS} = \dot{x}_2$, $\dot{T}_{POT} = \dot{x}_3$, $\dot{T}_{water} = \dot{x}_4$ and $P = u$, then the system is given in the equation 2:

$$\dot{x} = Ax + Bu \quad (2)$$

Where:

$$A = \begin{bmatrix} \frac{-(h_{CA}+h_{GC})}{C_{COIL}} & \frac{h_{GC}}{C_{COIL}} & 0 & 0 \\ \frac{h_{GC}}{C_{GLASS}} & \frac{-(h_{GA}+h_{GC}+h_{PG})}{C_{GLASS}} & \frac{h_{PG}}{C_{GLASS}} & 0 \\ 0 & \frac{h_{PG}}{C_{POT}} & \frac{-(h_{PA}+h_{PG}+h_{PW})}{C_{POT}} & \frac{h_{PW}}{C_{POT}} \\ 0 & 0 & \frac{h_{PW}}{(M_{water})CW} & \frac{-(h_{WA}+h_{PW})}{(M_{water})CW} \end{bmatrix}$$

$$B = \begin{bmatrix} \frac{1-k1}{C_{COIL}} \\ 0 \\ \frac{k1}{C_{POT}} \\ 0 \end{bmatrix}; \quad C = \begin{bmatrix} 0 & 0 & 1 & 0 \end{bmatrix}; \quad D = 0$$

4.2 Controller design

With PIDTune of simulink the controller design is realized. The plant behavior was determined by a field study realized in october 2019. The final constants that allow an adequate output are presented below, it is emphasized that the resulting control is definitely an integrator.

$$K_p = 0$$
$$K_i = 0.0003279$$
$$K_d = 0$$

According to the response obtained in simulation (Figure 6), the temperature behavior responds to the raised reference, in this case $95°C$ in an approximate time of 2.72 hours. In addition, the absence of oscillations is perceived providing a desired behavior.

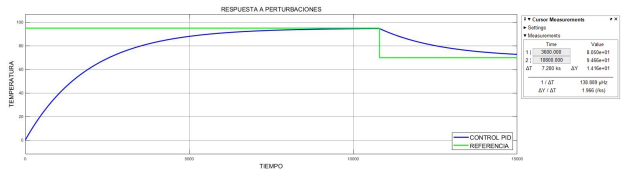

Figure 6 System output with integral control

The figure 7 present the simulation results with 2 disturbances. The system maintains stability and asymptotic tracking under the effect of disturbances. The average stabilization time is around 47 minutes, which in terms of toquilla straw production is acceptable.

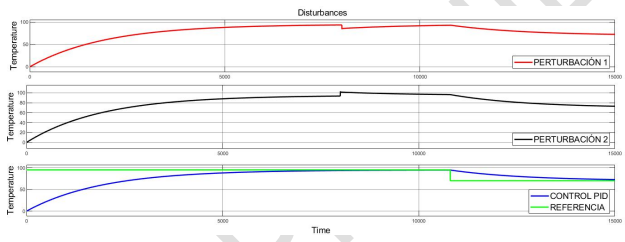

Figure 7 System output with disturbances

5. Design of the PV generator

The total power consumed by the stove is 4494 W and the toquilla straw cooking lasts 4 hours. Therefore, in the equation 3 is calculated the energy demanded by the stove is $17.97KWh$, taking a loss factor of 1.3 the real energy demanded is 23.36 KWh.

$$E_{CA} = (P)(t) \tag{3}$$

$$E_{CA} = (4494W)(4h) = 17,97KWh$$

$$E_{dm} = (17,974KW)(1.299) = 23,36KWh$$

In accordance of the calculation method presented in [10], the consumption must be change from kWh to Ah. Hence, the operating DC voltage selected is 48 V and the new demand is calculated in the equation 4.

$$Q = \frac{23,36KW}{48V} = 486,66Ah \tag{4}$$

The current to be generated by the PV system is calculated with Q and the incident irradiance in the zone or the Peak Sun Hours per day. For the calculation this value is $4.75h$ that is the minimum irradiance in Linares at the year, this current is calculated by the equation 5.

$$I_p = \frac{Q}{HSD_{crit}} = \frac{486,66Ah/dia}{4.75} = 102,45Ah/dia \tag{5}$$

PV modules of 400W are selected to minimize the amount of modules needed. The table 1 present the data of the module.

Table 1 PV module data

Variable	value
Power	400W
Voltage	24V
Current	9.6A
Efficiency	12-17 %
Type	Polycrystalline

The number of photovoltaic modules is determined from the analysis of the series and parallel configuration calculated by the equation 6,7 and 8, considering the degradation factor. The equation 6 determines the number of panels for a parallel configuration.

$$Np_{parallel} = \frac{I_p}{(F_d)(I_{operation})} \tag{6}$$

Where:

- $Np_{parallel}$ = Number of modules in parallel
- I_p = current generated by the panels
- F_d = Degradation factor
- $I_{operation}$ = Operating current of each module

$$Np_{parallel} = \frac{102,45A}{(0,9)(9,60A)}$$

$$Np_{parallel} = 11,85 = 12$$

$$Np_{series} = \frac{Vn}{Vn_p} = \frac{48V}{24V} \tag{7}$$

$$Np_{series} = 2$$

From the results above, the total number of PV modules is calculated as shown.

$$N_{Tp} = Np_{serie} Np_{paralelo} = (2)(12) = 24 \tag{8}$$

5.1 Inverter selection

According to [10] the sizing for inverters depends on the nominal voltage and the nominal power. On the other hand, the nominal power depends on the criterion of simultaneity, where the sum of all the powers of the receivers or loads that can operate simultaneously do not exceed the nominal power of the inverter. According to [10] assuming the critical case previously exposed, it is advisable to assign a simultaneity factor of 100%. The equation 9 determines the power value for an inverter according to the maximum load power and the safety factor in this case of 1.

$$P_{inv} = P_{AC} FS \tag{9}$$

$$P_{inv} = (4494W)(1) = 4494W$$

The characteristics of the selected inverter are presented in the table 2.

Table 2 Inverter EP18-5048 MUST Features

Inversor EP18-5048 MUST	
Potencia Máxima	5000W
Tensión nominal	48V
Voltaje de inversor	110/120V
Frecuencia de inversor	50/60Hz
Salida de onda sinusoidal	110/1120V

Finally, the Figure 8 shows the single-line diagram of the designed PV system.

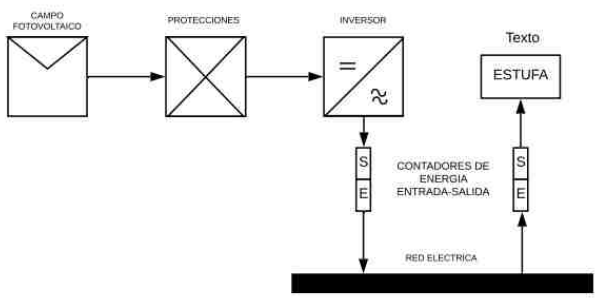

Figure 8 Single-line Schematic

6. Conclusions

The design of an induction stove with a temperature control and the support of an on-grid photovoltaic system is presented. The design for the modernization of a production process that is currently carried out in an artisan way in the municipality of Linares Nariño stands out as an important contribution, with which it is a matter of giving a contribution to the improvement of the production conditions of toquilla straw.

In addition, the temperature control of the system is remarkable. This control allow a temperature variation in a wide range, this is important in the toquilla straw production process. However, the stove designed and the control implemented can be applied to another productive process that is carried out by hand.

The implementation of an induction stove for this type of process brings an additional benefit and is the reduction in the use of firewood. The continuous use of firewood is not only an environmental impact but also generates health problems for people who are in constant contact with the process. The proposed design is presented as a contribution to the solution of these two problems that currently affect the study area and toquilla straw producers.

7. Declaration of competing interest

We declare that we have no significant competing interests including financial or non-financial, professional, or personal interests interfering with the full and objective presentation of the work described in this manuscript.

8. Acknow ledgdments

We thank the electronic engineering program of the Autonomous University Corporation of Nariño (AUNAR) for the technical and research support provided.

References

[1] E. comercio, "En 2020 se mantendrá subsidio para cocinas de inducción; el beneficio llega a 635000 hogares," https://notimundo.com.ec, 2019.

[2] M. S. Sánchez Álvarez, "Modelación y control de un sistema piloto de calentamiento de fluidos por inducción magnética," 2009.

[3] E. A. Cushicóndor Collaguazo Elías Antonio, "Diseño y construcción de un prototipo de una cocina de inducción electromagnética," 2009.
[4] S. y. S. C. y. A. O. Paesa, David y Llorente, "Observadores adaptativos aplicados al control de la temperatura de la olla de las placas de inducción," *IEEE Transactions on Industry Applications*.
[5] A. T. Franco, "Cocina de inducción versus cocina a gas (glp)," https://www.dspace.espol.edu.ec/bitstream/123456789/25742/1/Cocina%20de%20Inducci%C3%B3n%20versus%20Cocina%20a%20Gas%20%28GLP%29.pdf, 2013.
[6] D. J. Weber *et al.*, "Design of a battery-powered induction stove," Ph.D. dissertation, Massachusetts Institute of Technology, 2015.
[7] M. E. M. y. A. E. John N. Hincapié, Adriana Trejos, "Electrónica de potencia para el calentamiento por inducción doméstico: revisión del estado del arte," *http://www.eafit.edu.co/ingciencia*, vol. 9, pp. 237–262, 2013.
[8] J. M. A. Álvarez, "Inversores resonantes de alta frecuencia," http://ieee-pels-ies.es/Pels/Pdf/Inversores%20Resonantes.pdf, 1999.
[9] A. Boccuni, L. M. Capisani, F. Del Bello, D. De Vito, A. Ferrara, and J. Paderno, "Temperature estimation of cooking vessel content via ekf and sliding mode observers in induction cooking systems," *IFAC Proceedings Volumes*, vol. 44, no. 1, pp. 4350–4355, 2011.
[10] E. Mejía, "Diseño de un sistema fotovoltaico autónomo para el suministro de energía eléctrica al laboratorio de ingeniería mecánica de la universidad politécnica amazónica," *Revista Científica Pakamuros*, vol. 7, no. 2, pp. 73–88, 2019.